Comparison of in vivo contact positions for PS and PCR TKA implants using Lowest Point and full-contact techniques

Saikat Pal

University of Denver,
2390 S. York St.,
Denver, CO – 80208, USA
E-mail: spal5@stanford.edu

Mohamed R. Mahfouz

Mechanical, Aerospace, and Biomedical Engineering Department,
University of Tennessee,
307 Perkins Hall,
Knoxville, TN – 37996, USA
E-mail: mmahfouz@cmr.utk.edu

Richard D. Komistek

Mechanical, Aerospace, and Biomedical Engineering Department,
University of Tennessee,
301 Perkins Hall,
Knoxville, TN – 37996, USA
E-mail: rkomiste@utk.edu

Paul J. Rullkoetter*

Department of Engineering,
University of Denver,
2390 S. York, Denver, CO 80208, USA
Fax: 303.871.4450
E-mail: prullkoe@du.edu
*Corresponding author

Abstract: Evaluation of *in vivo* tibiofemoral contact following total knee arthroplasty provides valuable feedback to clinicians and researchers. The objective of the present study was to evaluate *in vivo* contact positions using a combination of fluoroscopy and Finite Element (FE) modelling. Center-of-Pressure (COP) contact locations from FE models were compared to Lowest Point (LP) results. Six P.F.C® Sigma Posterior Stabilised (PS) and 6 P.F.C® Sigma Posterior Cruciate Retraining (PCR) implants were analysed during weight-bearing knee flexion from 0° to 90°. Statistically significant differences were observed between the means of anterior-posterior contact position from the LP and COP methods ($\alpha = 0.05$).

Keywords: TKA; video fluoroscopy; tibiofemoral contact; knee kinematics; FE modelling; full-contact analysis; lowest point contact; COP; centre-of-pressure contact.

Reference to this paper should be made as follows: Pal, S., Mahfouz, M.R., Komistek, R.D. and Rullkoetter, P.J. (2011) 'Comparison of in vivo contact positions for PS and PCR TKA implants using Lowest Point and full-contact techniques', *Int. J. Biomedical Engineering and Technology*, Vol. 5, Nos. 2/3, pp.229–246.

Biographical notes: Saikat Pal received his BE in Computer Engineering, ME in Mechanical Engineering and PhD in Engineering from the University of Denver, USA. He is currently working as a post-doctoral scholar at Stanford University, USA. His research interests include computational modelling of musculoskeletal structures and application of probabilistic methods in biomechanics.

Mohamed R. Mahfouz received both his BS and MS in Systems and Biomedical Engineering from Cairo University, Egypt. He then received his second MS in Electrical Engineering from the University of Denver, Colorado, USA, before receiving his PhD in Systems Engineering from the Colorado School of Mines, Colorado, USA. He currently serves as a Career Development and Associate Professor in the Mechanical, Aerospace and Biomedical Engineering Department at the University of Tennessee, Knoxville, where he has been with the University since 2004. His research interests include surgical navigation, image processing, microelectromechanical systems, morphometric analysis, biomedical instrumentation, and 3D bone and tissue reconstruction.

Richard D. Komistek received his BS, MS and PhD in Mechanical Engineering from the University of Memphis, Tennessee, USA. He has been a Professor in the Mechanical, Aerospace and Biomedical Engineering Department at the University of Tennessee, Knoxville, since 2003 and was awarded the title of Fred M. Roddy Professor in 2007. His research interests include mathematical modelling, in vivo kinematic and kinetic analysis of the human body, design and analysis of total joint implantable devices, and closed and open loop control systems of the human body.

Paul J. Rullkoetter received his BSME from Duke University, and MS and PhD in Mechanical Engineering from Purdue University. He is currently an Associate Professor in the Department of Mechanical and Materials Engineering at the University of Denver, where he developed the Computational Biomechanics Lab. His current research interests include computational methods and joint biomechanics.

1 Introduction

Accurate knowledge of joint contact kinematics in vivo is important to evaluate the design and performance of total knee arthroplasty (TKA) devices. Numerous studies have utilised single- and dual-plane video fluoroscopy to acquire joint contact kinematics at the knee (Banks et al., 2003; Banks and Hodge, 1996; Banks et al., 1997; Bertin et al., 2002; Dennis et al., 1996, 1998a, 1998b, 2001a, 2001b, 2003; Fantozzi et al., 2003;

Hanson et al., 2006; Hoff et al., 1998; Komistek et al., 2002; Li et al., 2006; Machan et al., 2004; Nozaki et al., 2002; Schmidt et al., 2003; Stiehl et al., 1995; Wada et al., 2001; Walker, 2000; Walker et al., 1996). These studies have employed different techniques to estimate tibiofemoral contact position. The lowest point (LP) or closest point method, which estimates tibiofemoral contact location as the lowest or closest point on each femoral condyle relative to the tibial baseplate, has been used extensively to assess different implant designs (Banks et al., 1997, 2003; Bertin et al., 2002; Dennis et al., 1998a, 1996, 2003, 2001a). In a comprehensive study summarising the findings from more than 70 individual kinematic studies involving 811 normal and TKA knees, Dennis et al. (2004) applied the LP technique to conclude that substantial variability existed in kinematic patterns of the implants (Dennis et al., 2003a, 2003b). More recently, the centroids of the intersection areas of the femoral condylar surfaces with the tibial insert have been used to report in vivo contact (DeFrate et al., 2004; Hanson et al., 2006; Li et al., 2006). Using the centroid method, Li et al. (2006) reported anterior–posterior and medial–lateral contact on the tibial surface from dual-plane fluoroscopy (Li et al., 2006). DeFrate et al. obtained tibiofemoral anterior-posterior contact based on the centroid of overlap of cartilage layers in the natural knee and compared it to the lowest point contact between the bony surfaces (DeFrate et al., 2004).

Joint contact kinematics using the LP and centroid methods provide valuable information on the relative position of components in vivo; however, the effects of including surface geometry interactions on estimated contact locations are unclear (Figure 1). The addition of full-contact modelling to a fluoroscopic analysis accounting for implant conformity and surface interactions would prove beneficial. At present, there is limited data in the literature on the application of in vivo fluoroscopy kinematics to full-contact modelling techniques like finite element (FE) analysis. Walker (2000) incorporated in vivo kinematic data obtained from video fluoroscopy to two-dimensional sagittal plane FE models to estimate contact stresses on the tibial inserts during flexion. Fregly et al. (2005) employed fluoroscopy-derived kinematic data with three-dimensional FE modelling to predict wear of a single polyethylene insert, and compared the numerical results with the wear patterns on the same retrieved insert. Machan et al. (2004) compared the contact stresses obtained from dynamic FE models driven by gait curves with static FE models of the implants in a given pose captured from fluoroscopy images. To the best of our knowledge, methods utilised in reporting tibiofemoral contact locations from fluoroscopic analyses (such as LP or centroid methods) have not been compared with a full-contact technique.

A research question of particular interest necessitating video fluoroscopy has been the comparison of in vivo kinematics of fixed-bearing PS and PCR TKA implants (Banks et al., 1997; Dennis et al., 1998b; Komistek et al., 2002; Maruyama et al., 2004; Yoshiya et al., 2005). Studies have reported inconsistencies in kinematic performance of these two implant designs, including anterior femoral translation, posterior femoral rollback and variable cam-post engagement during flexion. From their comprehensive study, Dennis et al. (2003a, 2003b) reported certain trends associated with specific designs. For example, under weight-bearing knee flexion, anterior translation of the femoral component was commonly observed in PCR designs, whereas PS designs showed routinely greater femoral rollback, consistent with findings from separate studies (Dennis et al., 1998b, 2003a, 2003b; Yoshiya et al., 2005). In contrast, Bertin et al. (2002) reported consistent posterior femoral rollback observed in PCR implants during knee flexion. Also, numerous studies attribute steady rollback of the PS

femoral component at higher flexions (>60°) to consistent engagement of the cam-post mechanism (Dennis et al., 1998a, 1998b; Fantozzi et al., 2003; Komistek et al., 2002; Most et al., 2003; Wada et al., 2001). Results from the Dennis et al. study (Dennis et al., 2003a, 2003b), however, contradict these assertions, highlighting variability in rollback of PS femoral components, as well as cam-post engagement under flexion. It described fixed-bearing PS TKA implants that showed excessive posterior contact position throughout the flexion range, thereby never achieving cam-post engagement (Dennis et al., 2003a, 2003b).

Figure 1 Anterior–posterior location of contact using LP and COP methods

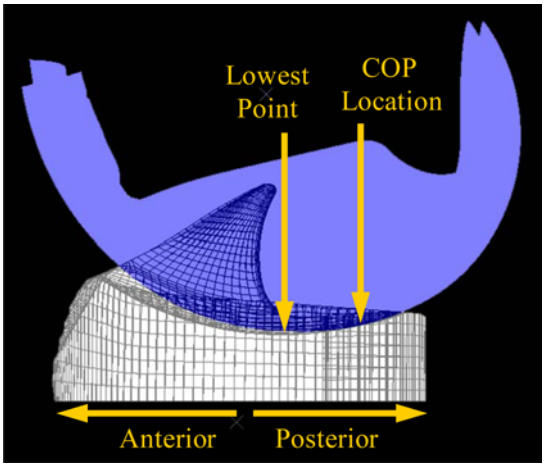

The objectives of this study were – (1) to develop a computational methodology to obtain *in vivo* tibiofemoral contact using a combination of video fluoroscopy and FE modeling, (2) compare tibiofemoral contact locations obtained from lowest point estimates and full-contact analyses, and (3) apply the methodology to compare kinematics of PS and PCR TKA implants.

2 Methods

Single-plane fluoroscopy data from 12 consenting TKA patients with fixed-bearing implants were used. Approval was obtained from an Institutional Review Board prior to performing the study (Rose Medical Center #0445). Six patients had P.F.C® Sigma PS implants, and 6 had P.F.C® Sigma PCR (semi-constrained) implants (DePuy Orthopedics, Warsaw, IN). The implant designs were identical in geometry except for the presence of a cam, box and post in the PS design. All implants were determined to be clinically successful, with no ligamentous laxity or pain, and Hospital for Special Surgery knee scores rated in the excellent category (>90).

Patients were requested to perform a weight-bearing knee bend to maximum flexion under fluoroscopic surveillance. The knee bend was performed with feet staggered so that the non-implanted knee did not obscure the implanted knee and the fluoroscopy machine. Fluoroscopic images from 0° to 90° flexion, at 10° intervals, were digitised for each implant in the sagittal plane (Figure 2(a)). Computer-Aided Design (CAD) models

of the implants were overlaid on the images using an interactive three-dimensional to two-dimensional model-fitting technique (Hoff et al., 1998). For each image, the position and orientation of the femoral and tibial components with respect to the fluoroscopy machine (Radiographic and Data Solutions, Inc., Minneapolis, MN) were extracted (Figure 2(b)). The geometric centres of the components were used as their local reference origins. Reported errors for the model-fitting process are less than 0.5 mm for in-plane translations (anterior–posterior and inferior–superior directions in the sagittal plane) and less than 0.5° for all rotations (Dennis et al., 2003a, 2003b).

Figure 2 Process of transforming video fluoroscopy images to kinematic data for input to an FE model: (a) digitised image of an implant from fluoroscopy; (b) three-dimensional model fitting to obtain relative implant pose; (c) FE model of the implant using six degrees-of-freedom kinematics obtained from model fitting; (d) the model under a combination of joint loading and fluoroscopic kinematic variables to account for component over-closures observed in (c)

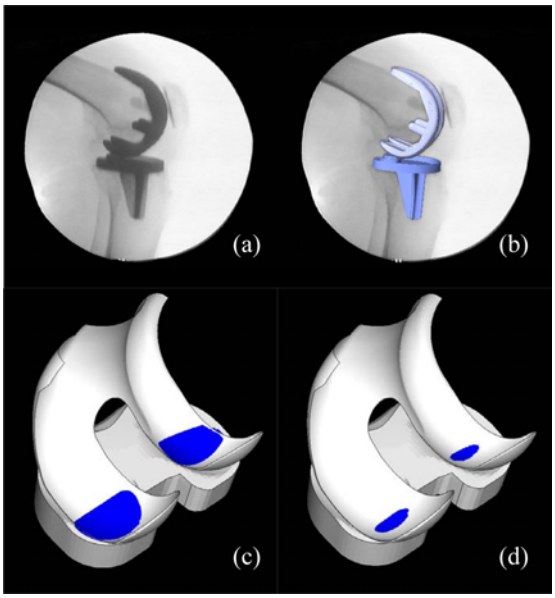

An FE model of the femoral component contacting the polyethylene insert was created in ABAQUS™/Explicit (Simulia, Providence, RI) (Figure 3). An explicit FE model was selected for its efficiency in estimating tibiofemoral contact under dynamic, large-displacement conditions. The femoral component was modelled as three-dimensional surface elements, and 8-noded hexahedral elements were used to represent the polyethylene insert. The average edge length for the femoral and tibial component meshes were ~1 mm and ~1.5 mm, respectively. The femoral and tibial components were represented as rigid bodies. Unlike a standard FE analysis performed to evaluate internal stresses, the emphasis of this study was to estimate surface contact locations; as such, the rigid body assumption was appropriate and greatly improved the computational efficiency of the FE model. Contact was defined using a previously verified non-linear pressure-overclosure relationship (Halloran et al., 2005), a penalty-based method with a

weight factor where contact forces were evaluated as a function of the penetration distance of the master into the slave surface.

Figure 3 FE model of a P.F.C® Sigma posterior stabilising implant illustrating applied boundary conditions. The tibia was fixed in all 6 degrees of freedom. For the femoral component, in vivo fluoroscopy data were used to specify anterior–posterior, internal–external and flexion–extension displacements, while medial–lateral and varus–valgus Degrees Of Freedom were unconstrained. A compressive load was applied to the femoral component to maintain contact in the medial and lateral condyles throughout the knee flexion cycle

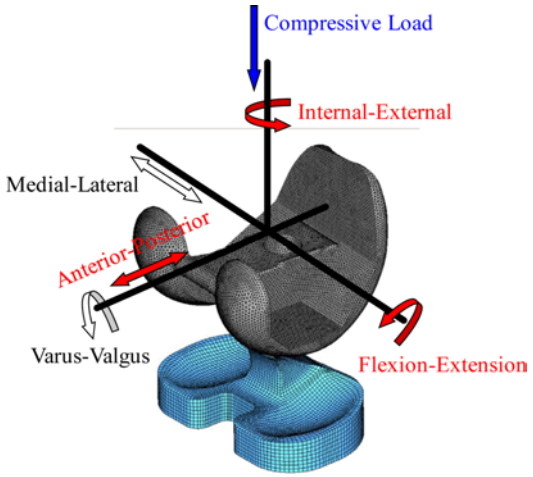

A combination of kinematic degrees of freedom derived from fluoroscopy and joint loading was used as boundary conditions to the FE models. The tibial insert was fixed, and all boundary conditions were applied to the femoral component. Fluoroscopic kinematic data were used to specify anterior–posterior translation, and internal–external and flexion–extension rotations to the femoral component (Figure 3). Medial–lateral and varus–valgus degrees of freedom were unconstrained (Fregly et al., 2005). To remove potential over-/under-closures (Figure 2(c)), the initial position of the femoral component was modified in the inferior–superior direction, and a constant compressive load of 750 N (estimating one bodyweight) was applied to maintain contact during the range of flexion (Figures 2(d) and 3). The compressive load is applied to maintain contact between the femoral component and the tibial insert, and its magnitude will not influence the location of tibiofemoral contact in these analyses. This combination of joint loading and kinematic variables accounted for potential over-/under-closures owing to the tolerances in model-fitting (Dennis et al., 2003a, 2003b), and provided continuous contact on the medial and lateral condyles throughout the knee flexion cycle.

Tibiofemoral anterior–posterior contact positions from two different methods were compared. Contact positions were obtained directly from a fluoroscopic analysis using the LP method – from the relative pose and model dimensions of an implant, the lowest inferior–superior point on each femoral condyle relative to the insert was denoted as the location of contact. From the FE models, condylar contact position was calculated from the COP location of contact patches on the polyethylene insert (Figure 2(d)).

In addition, to provide a direct comparison between the contact position-reporting methods on a single platform, condylar LP results were extracted from the FE models. Relative internal–external rotations based on anterior–posterior contact points were also calculated from the LP and COP methods. Lowest point data from the fluoroscopic analysis were obtained at every 10° knee flexion, while results from the FE models were extracted at 1° intervals.

The computational time for a single FE analysis was approximately 2 min. Analysis of variance (ANOVA) using single factor was performed to test the means of the LP and COP contact positions. The level of significance (α) was set to 0.05.

3 Results

Tibiofemoral anterior–posterior contact positions for the 6 PS and 6 PCR implants were determined using the LP and COP methods. Femoral contact anterior to the mid-coronal plane of the tibial articular surface was denoted as positive, whereas posterior contact was denoted as negative. Internal–external rotation based on condylar anterior–posterior contact location was also calculated. Femoral external rotation was denoted as positive, and internal rotation was denoted as negative.

3.1 Comparison of Lowest Point and Centre-of-Pressure contact methods

Substantial variability in anterior–posterior contact position was observed from the LP and COP methods for the PS and PCR implants (Figure 4). For the PS implants, the ranges of anterior–posterior position were 10.8 mm (medial) and 7.9 mm (lateral) using the LP technique, compared with 15.1 mm (medial) and 16.4 mm (lateral) from the COP method (Figure 4(a)–(d)). For the PCR implants, the ranges of anterior–posterior position were 14.7 mm (medial) and 10.4 mm (lateral) using the LP technique, and 25.7 mm (medial) and 14.9 mm (lateral) from the COP method (Figure 4(e)–(h)).

Mean COP contact locations from FE modelling were generally farther posterior than the LP data (Figure 5). Contact location from the COP method was, on average, 3.4 mm (medial) and 1.8 mm (lateral) posterior to the LP for the PS implants (Figure 5(a) and 5(b)), and 0.7 mm (medial) and 0.3 mm (lateral) for the PCR implants (Figure 5(c) and 5(d)) throughout the flexion cycle. The difference in contact between the two methods was largest during the first 30° flexion, with the average initial femoral rollback from the LP method being 1.9 mm, compared with 5.7 mm from the COP technique (Figure 5). Standard deviations associated with the contact locations using FE COP were typically larger than those obtained from the fluoroscopic LP method (Figure 5). For the PS implants, the maximum standard deviations were 2.8 mm (medial) and 2.2 mm (lateral) from LP, compared with 4.7 mm (medial) and 4.3 mm (lateral) from COP. For the PCR implants, the maximum standard deviations were 4.3 mm (medial) and 3.2 mm (lateral) from the LP method, and 10.3 mm (medial) and 4.1 mm (lateral) from the COP method. There were statistically significant differences between the means of anterior–posterior contact position between the two methods. For the PS implants, statistically significant differences were observed throughout the flexion cycle in the medial condyle (Figure 5(a)), and from 10° to 40° in the lateral condyle (Figure 5(b)).

For the PCR implants, statistically significant differences were observed in the lateral condyle at 10° and 90° knee flexion (Figure 5(d)).

Figure 4 Anterior–posterior Lowest Point (LP) and Centre-of-Pressure (COP) contact position from fluoroscopy and FE analysis (FEA), respectively, for the six Posterior Stabilised (PS) (a)–(d) and six Posterior Cruciate Retaining (PCR) (e)–(h) implants. The LP estimates from the fluoroscopic analysis were evaluated at every 10°, while the COP results were extracted at 1° intervals from FEA (see online version for colours)

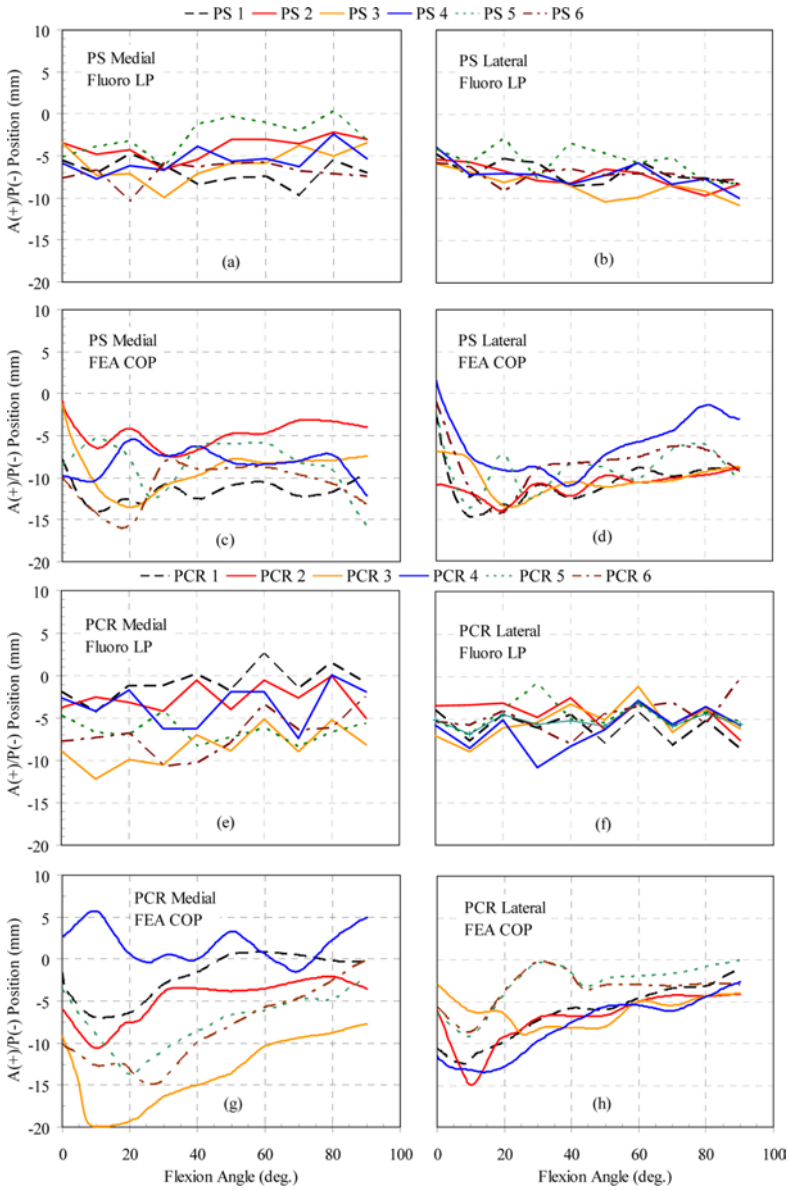

Figure 5 Average anterior–posterior Lowest Point (LP) and Centre-of-Pressure (COP) contact positions from fluoroscopy and Finite Element Analysis (FEA) for the Posterior Stabilised (PS) (a) and (b) and Posterior Cruciate Retaining (PCR) (c) and (d) implants. Error bars represent 1 standard deviation. The ● represents statistically significant differences between Fluoro LP and FEA COP, while ■ represents statistically significant differences between FEA LP and FEA COP ($\alpha = 0.05$) (see online version for colours)

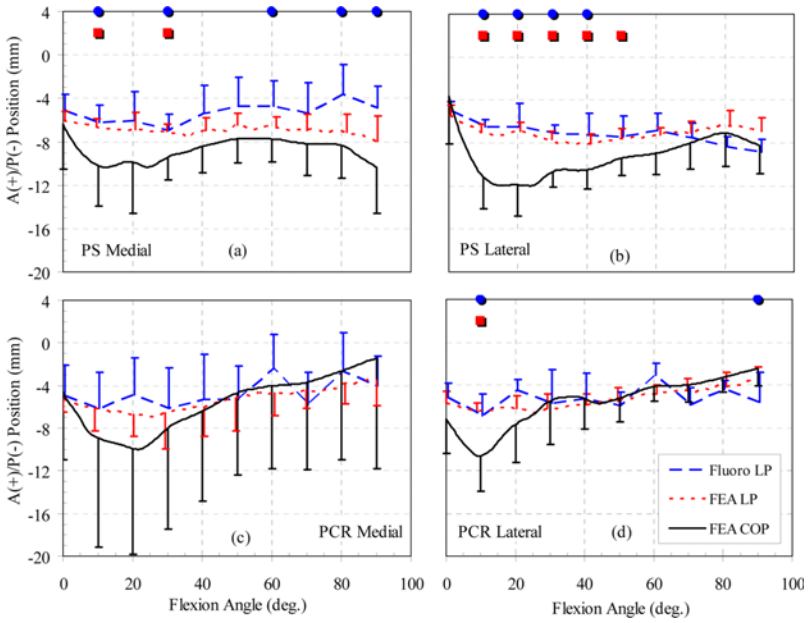

A direct comparison of anterior–posterior contact position using the COP and LP methods obtained from the FE models yielded similar greater posterior contact using the COP method (Figure 5). COP contact, on average, was 1.8 mm (medial) and 1.9 mm (lateral) posterior to the LP location for the PS implants, and 0.2 mm (medial and lateral) posterior for the PCR implants. Consistent with the LP results reported directly from the fluoroscopic evaluation (Figure 5), LP data from FE modelling displayed minimal initial (from 0° to 30°) femoral rollback as well as smaller standard deviations than the COP results (Figure 5). Statistically significant differences between the means of anterior–posterior contact position were observed at lower flexion angles for both the implant designs (Figure 5).

In general, average internal–external rotations calculated from condylar anterior–posterior contact points were comparable between the LP and COP methods, with statistically significant differences observed only beyond 80° flexion in the PS implants (Figure 6). The ranges of average internal–external rotation were 6.5° (LP) and 4.9° (COP) for the PS implants (Figure 6(a)), and 2.9° (LP) and 6.2° (COP) for the PCR implants (Figure 6(b)). As with the anterior–posterior contact location, the COP method demonstrated greater variability in internal–external rotation than the LP method, with maximum standard deviations from the COP method being 8.5° (PS) and 15.6° (PCR), compared with 4.0° (PS) and 6.0° (PCR) from the LP technique. Statistically significant differences between the means of internal–external rotations were observed at 80° and 90° flexion in the PS implants (Figure 6).

Figure 6 Average internal–external rotation of tibiofemoral contact using Lowest Point (LP) and Centre-of-Pressure (COP) locations from fluoroscopy and Finite Element Analysis (FEA), respectively, for the (a) Posterior Stabilised (PS) and (b) Posterior Cruciate Retaining (PCR) implants. Error bars represent 1 standard deviation. The ● represents a statistically significant difference between the methods ($\alpha = 0.05$) (see online version for colours)

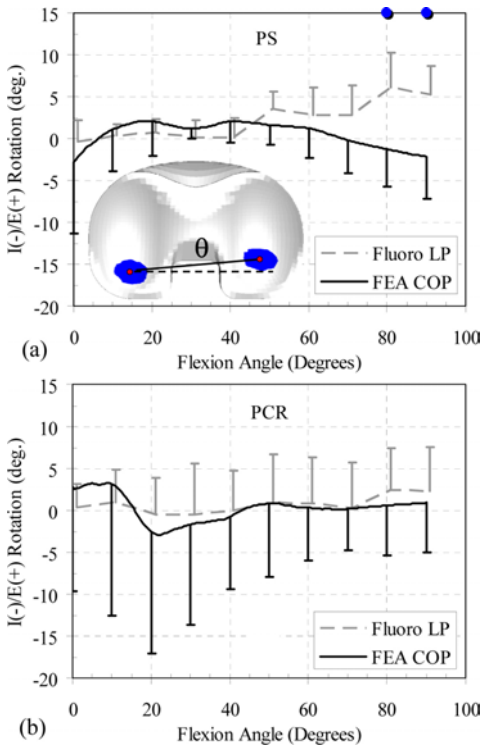

3.2 Comparison of PS and PCR implant contact location using Centre-of-Pressure method

Substantial differences in anterior–posterior contact position were observed between the implant designs using the COP method. For the PS implant, the range of anterior–posterior position for the medial and lateral condyle was 15.1 mm and 16.4 mm, respectively (Figure 4(c) and (d)). After initial rollback, the lateral condyles translated anteriorly, with maximum anterior slide being 9.6 mm (Implant 4). Femoral rollback at flexion angles greater than 60° was observed in 3 PS implants (Implants 4, 5 and 6; Figure 4(c) and (d)). For the PCR implants, the range of anterior–posterior position for the medial and lateral condyle was 25.7 mm and 14.9 mm, respectively (Figure 4(g) and (h)). Beyond 10° flexion, the condyles generally displayed steady anterior sliding on the polyethylene insert, with maximum anterior slide of 14.8 mm (Implant 6) for the medial condyle, and 11.4 mm (Implant 1) for the lateral condyle. Posterior femoral rollback at higher flexion angles (>60°) was not observed in any PCR implant (Figure 4(g) and (h)).

On average, the PS design yielded greater posterior contact with flexion than the PCR design (Figures 7 and 8). There were statistically significant differences between the

means of anterior–posterior contact position of the PCR and PS designs from 70° to 90° for the medial condyle, and 20° to 90° for the lateral condyle (Figure 7). From 0° to 20°, the average contact position of the lateral condyle of the PS design and the medial condyles of both designs displayed posterior rollback. From 20° to 80°, the average contact position moved anteriorly, with the rate of anterior translation for the medial and lateral condyles being 0.11 ($R^2 = 0.94$) and 0.06 ($R^2 = 0.91$) mm per degree flexion, respectively (PCR), and 0.04 ($R^2 = 0.71$) and 0.08 ($R^2 = 0.98$), respectively (PS). Beyond 80° flexion, average contact position for the PCR design slid further anteriorly, whereas contact position of the PS design demonstrated posterior femoral rollback (Figure 7).

Figure 7 Average anterior–posterior Centre-of-Pressure (COP) contact position from Finite Element Analysis for (a) medial, and (b) lateral condyles of the Posterior Stabilised (PS) and Posterior Cruciate Retaining (PCR) implant designs. Error bars represent 1 standard deviation. The ● represents a statistically significant difference between the implant designs ($\alpha = 0.05$) (see online version for colours)

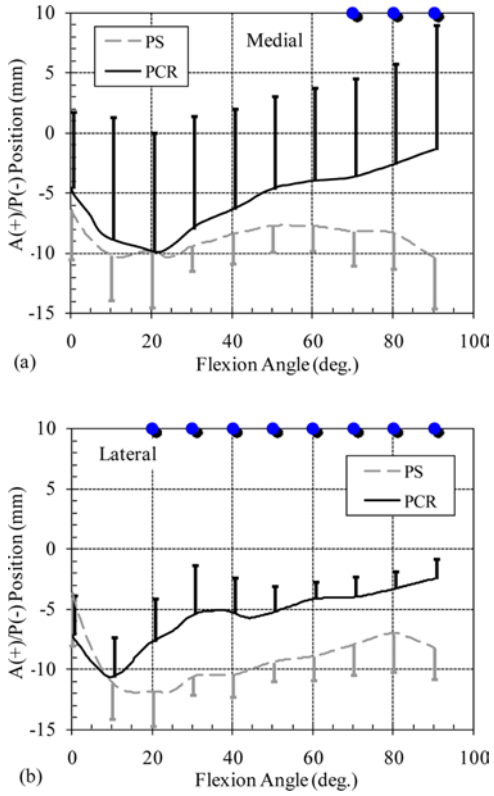

Overall, the PCR design demonstrated greater variability in anterior–posterior contact position than the PS design (Figure 7). Throughout the range of flexion, the maximum standard deviation for the PCR implant was 8.5 mm, compared with 4.7 mm for the PS design. Within the PCR implants, anterior–posterior contact position variability on the medial condyle was greater than the lateral condyle (Figure 7). The maximum standard deviation of the PCR medial condyle was 8.5 mm, compared with 4.1 mm for the PCR

lateral condyle. Variability between the condyles of the PS design was similar, with maximum standard deviations being 4.4 mm and 4.7 mm for the medial and lateral condyles, respectively.

Figure 8 Composite Centre-of-Pressure (COP) contact area of representative Posterior Stabilised (PS) and Posterior Cruciate Retaining (PCR) implants during knee flexion from 0° to 90° (see online version for colours)

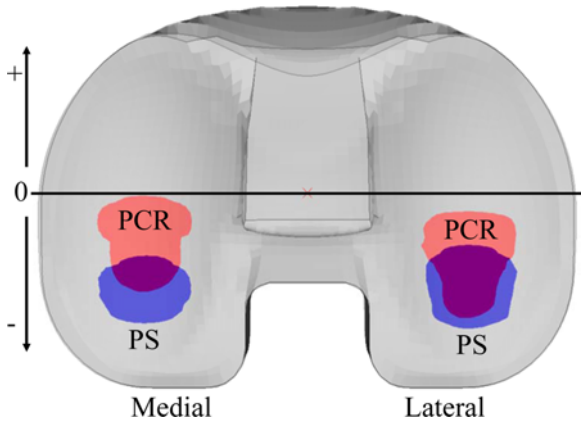

For the range of flexion evaluated, engagement of the femoral cam on the tibial post was not observed in any of the PS implants, as the femoral component was too far posterior on the tibial insert to contact the post. In two cases (Implants 2 and 4), the ML boundary of the cam box contacted the edge of the post due to IE rotation, but direct engagement of the cam and post (to restrict anterior sliding of the femoral component on the insert) was not observed (Figure 4(c) and (d)).

4 Discussion

Functionality and survivorship of TKA devices are contingent on joint kinematics during in vivo physiological activity. Contact position data for the components serve as indicators of potential performance of the implanted knee. Kinematic abnormalities have been shown to greatly affect the success of TKA components, and numerous studies have documented that many of these patient- and implant-design-specific variances are not observed unless testing is done under in vivo, weight-bearing conditions (Dennis et al., 1996, 1998b; Hsieh and Walker, 1976). Video fluoroscopy allows analysis of TKA implants under these conditions. Studies utilising lowest or closest point methods represent efficient techniques to acquire valuable information on the relative position of components in vivo (Banks and Hodge, 1996; Banks et al., 1997; Dennis et al., 1998b, 2003a, 2003b; Hanson et al., 2006; Li et al., 2006); however, these methods do not include surface geometry interactions when estimating contact location. The addition of full-contact modelling incorporates the effects of geometric conformity and surface interactions in assessing joint contact location. As such, fluoroscopy combined with a full-contact modelling technique like FE analysis is beneficial for obtaining joint contact in vivo.

A combination of joint loading and fluoroscopic kinematic variables was used as inputs to the FE models to obtain appropriate COP contact results. The compressive-loaded models incorporated important in vivo boundary conditions – anterior–posterior, internal–external and flexion–extension displacements, while masking the inferior–superior, medial–lateral and varus–valgus kinematics obtained from fluoroscopic analysis. It is important to note that the results from the FE models reported in this study – the anterior–posterior and internal–external contact location as a function of knee flexion – were the degrees of freedom in the FE models that were directly controlled by the extracted fluoroscopic kinematic data. This modelling methodology is capable of accommodating any combination of in vivo kinematic data or joint loading to obtain additional information such as potential condylar lift-off.

Results from this study suggest that there may be significant differences between the location of LPs on the femoral condyles and the COP contact positions, with the latter generally being further posterior for the two implant designs evaluated (Figures 4 and 5). In both the PS and the PCR designs, initial femoral rollback was observed causing the COP contact locations to move posterior (Figure 5). The effects of this initial femoral rollback were minimal on the LP locations, resulting in statistically significant differences in contact positions between the two methods. Standard deviations associated with anterior–posterior contact positions from FE COP results were typically larger than those obtained from the LP method (Figure 5). The largest standard deviation from the COP method was 10.3 mm from the medial condyle of the PCR design, compared with 4.3 mm using the LP method (Figure 5). Reported anterior–posterior contact position variability was greater using the FE COP method primarily because when accounting for surface conformity, small changes in tibiofemoral position may lead to large changes in predicted contact location without substantially affecting the position of the condylar LP.

In addition to the comparison of contact position using LP and COP methods from fluoroscopic analysis and FE modelling, respectively, LP data were also extracted from the FE models (Figure 5). While the LP data from the fluoroscopy analysis were based on the six degrees-of-freedom position and orientation of components, the FE LP results were obtained from models with a combination of in vivo kinematics and joint loading as boundary conditions. This explains the differences in LP contact locations obtained from fluoroscopy and FE modelling (Figure 5). A direct comparison between the COP and LP methods using identical boundary conditions within this single FE platform clearly highlights the differences in contact locations obtained from LP estimates and full-contact analyses.

Although the means of internal–external rotation of contact points displayed minimal ranges (Figure 6), substantial internal–external rotations were observed in individual implants during knee flexion. While the mean internal–external rotation ranged from –2.8° to 2.1° (PS) and –3.0° to 3.2° (PCR) (Figure 6), maximum internal–external rotations from the six PS and six PCR implants were –12.1° to 10.0° and –17.1° to 31.3°, respectively, from the FE COP contact positions (not shown). Consistent with anterior–posterior contact results, the COP data displayed greater variability in internal–external rotation than the LP method owing to the sensitivity of contact location to a conforming implant geometry.

Comparison of PS and PCR implants using the COP contact method suggested that the retention of the PCL did not necessarily mean retaining its function. Previous studies have advocated the retention of PCL to increases in moment arm, range of motion, mechanical efficiency of the knee musculature, and restoration or maintenance of

proprioception after TKA (Simmons et al., 1996; Warren et al., 1993). Further, the retention of the PCL in TKA theoretically improves the efficiency of the extensor mechanism, prevents subluxation of the tibia on the femur and permits natural femoral rollback during knee flexion (Schmidt et al., 2003; Sorger et al., 1997). In this study, however, femoral rollback owing to the retention of the PCL was not observed at higher flexion angles (> 60°) (Figure 4(a) and (b)). Instead, the condyles of the PCR implants displayed a steady anterior slide with flexion. This paradoxical anterior sliding was minimal in the PS implants, and hence, the more posterior contact of the PS condyles throughout the range of flexion (Figure 4(c) and (d)).

There are potentially several detrimental effects of anterior sliding seen in the PCR implant type, as reported by Dennis et al. (2003a, 2003b). Anterior femoral translation results in a more anterior axis of flexion, reducing maximum range of motion. The quadriceps moment arm is decreased, and anterior sliding of the femoral component on the tibial surface risks accelerated polyethylene wear (Blunn et al., 1991; Dennis et al., 2003a, 2003b; Hoff et al., 1998). The cause of this anterior translation may be related to soft-tissue balancing. Owing to lack of adequate tension in the PCL, it poorly resists the backward directed shear force on the tibia from the tightening of the extensor mechanism during flexion (Dennis et al., 1996, 2003a, 2003b; Wada et al., 2001). Studies in the past have reported femoral rollback in appropriately balanced PCL retaining knee replacements; however, as this study indicates, it is difficult to achieve suitable ligament tensions consistently.

Kinematic patterns observed in the PS design at higher flexion angles may not be necessarily governed by cam-post interaction. Steady rollback of the PS femoral component at high flexion has been attributed to consistent engagement of the cam-post mechanism (Dennis et al., 1998a, 1998b; Fantozzi et al., 2003; Komistek et al., 2002; Most et al., 2003; Wada et al., 2001). The findings of this study are different in two ways. First, it does not support the assertion that the PS implants display consistent rollback at higher flexions. Implants 1, 2 and 3 do not display femoral rollback beyond 10° (Figure 4(c) and (d)). This is in agreement with the findings from Dennis et al. (2003a, 2003b). Second, femoral rollback observed in the PS implant design at higher flexion angles may not be due to cam-post interaction (Figure 4(c) and (d)). Three PS implants displayed femoral rollback at flexions beyond 60°, but they were not a result of cam-post engagement, as the femoral components were too far posterior on the tibial insert. The femoral component and tibial insert used in the two implant types were identical in geometry except for the presence of the cam, box and post in the PS design. Therefore, femoral rollback in the three PS implants may be due to differences in surgical technique (when compared with the PCR design that showed no femoral rollback, but had similar conforming polyethylene geometry), or soft-tissue balancing. As several previous studies report, it is difficult to achieve consistent and appropriate PCL strains to reproduce rollback in the PCR TKA (Incavo et al., 1994; Mahoney et al., 1994; Nozaki et al., 2002). The resection of the PCL in PS TKA may lead to the simplification of the surgical technique, facilitating more frequent rollback at higher flexions.

Results from this study are consistent with previously documented in vivo analyses. Numerous studies have shown that contact of the femoral component on the tibial insert is mostly posterior, with contact for the PS implant type being significantly more posterior than the PCR (Banks et al., 1997, 2003; Dennis et al., 1996, 1998a, 1998b, 2001a, 2001b, 2003a, 2003b). Experiments under unloaded conditions carried out by Most et al. (2003) reported that femoral rollback was regularly seen in the PCR implant

type with flexion. From 60° to 90°, the average femoral rollback of the lateral condyle was around 5 mm. In one group of PCR implants under weight-bearing deep flexion, Nozaki et al. (2002) observed femoral rollback of 8.8 mm and 6.8 mm for the lateral and medial condyles, respectively. However, a second group of the same implant type under similar conditions displayed bicondylar anterior sliding of approximately 6 mm from 20° to 80°. The current study suggests an anterior slide of both condyles of the PCR during knee bend. The differences in kinematics under weight-bearing and non-weight-bearing conditions may account for the discrepancies with the Most et al. study, whereas variations in ligament balancing and surgical techniques account for disparities between the groups in the Nozaki study. Next, there is high variability in kinematic patterns like AP translation and IE rotation, and in general, the variability is greater in the PCR implant type. This is supported by previous studies (Banks et al., 1997; Komistek et al., 2002), and may again be due to differences in surgical techniques and soft-tissue balancing.

Limitations of this study include the relatively small number of implants evaluated (6 PS and 6 PCR). A more comprehensive study with a greater number of implants would assist in better understanding of kinematic variances observed between the implant designs. Kinematic data were obtained from a single-plane fluoroscope, hence medial–lateral contact location could not be reported as in the Li et al. study (2006), and only one activity (weight-bearing knee flexion) was analysed. The methodology could readily accommodate the 6 degrees-of-freedom data from dual-plane fluoroscopy, as well as evaluate other activities like gait, stair ascent/descent and knee bend beyond 90° to capture the range of kinematic conditions that an implant encounters. This study does not address the potential differences in tibiofemoral contact position between the COP and centroid methods; a future study comparing these two methods would be beneficial. Although a full-contact modelling technique like FE analysis provides additional capabilities such as the estimation of contact pressures or even potential wear performance, the tolerances associated with model-fitting as well as intrinsic differences in using an unworn CAD model to represent an in-service implant may make it difficult to obtain reliable predictions.

This study presents a novel approach to obtain in vivo joint contact kinematics using a combination of fluoroscopy data and FE modelling. Tibiofemoral contact position from the COP and LP methods were compared. Statistically significant differences in contact locations were observed between the two techniques, with contact from the COP method being farther posterior than the LP. The differences in estimated LP and COP contact locations would be greatest for high conformity implant designs, highlighting the importance of a full-contact modelling technique. At the same time, the larger standard deviations associated with the COP results were due to the effects of surface interactions on tibiofemoral contact location. Whereas the COP method was sensitive to geometric conformity, the LP method was insensitive to such interactions and provided an efficient estimate of the relative position of the implant components. The FE-based COP method was used to compare contact positions between PS and PCR implants. The PS implant demonstrated significantly greater posterior contact than the PCR design. Femoral rollback was observed in 3 PS implants, whereas the condyles of the PCR implants displayed steady anterior sliding with flexion. Cam-post engagement was not observed in any of the PS implants in the flexion range evaluated. A combination of fluoroscopic analysis and FE modelling incorporates surface interactions and geometric conformity when determining joint contact, and can be a valuable addition to a traditional

fluoroscopic analysis evaluating patient- and implant-design-specific joint contact kinematics under in vivo weight-bearing conditions.

Acknowledgements

This research was supported in part by DePuy, a Johnson & Johnson Company, and Rocky Mountain Musculoskeletal Research Laboratory.

References

Banks, S., Bellemans, J., Nozaki, H., Whiteside, L.A., Harman, M. and Hodge, W.A. (2003) 'Knee motions during maximum flexion in fixed and mobile-bearing arthroplasties', *Clin. Orthop. Relat. Res.*, Vol. 410, pp.131–138.

Banks, S.A. and Hodge, W.A. (1996) 'Accurate measurement of three-dimensional knee replacement kinematics using single-plane fluoroscopy', *IEEE Trans. Biomed. Eng.*, Vol. 43**,** pp.638–649.

Banks, S.A., Markovich, G.D. and Hodge, W.A. (1997) 'In vivo kinematics of cruciate-retaining and -substituting knee arthroplasties', *J. Arthroplasty*, Vol. 12, pp.297–304.

Bertin, K.C., Komistek, R.D., Dennis, D.A., Hoff, W.A., Anderson, D.T. and Langer, T. (2002) 'In vivo determination of posterior femoral rollback for subjects having a NexGen posterior cruciate-retaining total knee arthroplasty', *J. Arthroplasty*, Vol. 17, pp.1040–1048.

Blunn, G.W., Walker, P.S., Joshi, A. and Hardinge, K. (1991) 'The dominance of cyclic sliding in producing wear in total knee replacements', *Clin. Orthop. Relat. Res.*, Vol. 273, pp. 253–260.

Defrate, L.E., Sun, H., Gill, T.J., Rubash, H.E. and Li, G. (2004) 'In vivo tibiofemoral contact analysis using 3D MRI-based knee models', *J. Biomech.*, Vol. 37, pp.1499–1504.

Dennis, D., Komistek, R., Scuderi, G., Argenson, J.N., Insall, J., Mahfouz, M., Aubaniac, J.M. and Haas, B. (2001a) 'In vivo three-dimensional determination of kinematics for subjects with a normal knee or a unicompartmental or total knee replacement', *J. Bone Joint Surg. Am.*, Vol. 83-A Suppl 2 Pt 2, pp.104–115.

Dennis, D.A., Komistek, R.D. and Mahfouz, M.R. (2003a) 'In vivo fluoroscopic analysis of fixed-bearing total knee replacements', *Clin. Orthop. Relat. Res.*, Vol. 410, pp.114–130.

Dennis, D.A., Komistek, R.D., Mahfouz, M.R., Haas, B.D. and Stiehl, J.B. (2003b) 'Multicenter determination of in vivo kinematics after total knee arthroplasty', *Clin. Orthop. Relat. Res.*, Vol. 416, pp.37–57.

Dennis, D.A., Komistek, R.D., Colwell Jr., C.E., Ranawat, C.S., Scott, R.D., Thornhill, T.S. and Lapp, M.A. (1998a) 'In vivo anteroposterior femorotibial translation of total knee arthroplasty: a multicenter analysis', *Clin. Orthop. Relat. Res.*, Vol. 356, pp.47–57.

Dennis, D.A., Komistek, R.D., Hoff, W.A. and Gabriel, S.M. (1996) 'In vivo knee kinematics derived using an inverse perspective technique', *Clin. Orthop. Relat. Res.*, Vol. 331, pp.107–117.

Dennis, D.A., Komistek, R.D., Stiehl, J.B., Walker, S.A. and Dennis, K.N. (1998b) 'Range of motion after total knee arthroplasty: the effect of implant design and weight-bearing conditions', *J. Arthroplasty*, Vol. 13, pp.748–752.

Dennis, D.A., Komistek, R.D., Walker, S.A., Cheal, E.J. and Stiehl, J.B. (2001b) 'Femoral condylar lift-off in vivo in total knee arthroplasty', *J. Bone Joint Surg. Br.*, Vol. 83, pp.33–39.

Fantozzi, S., Benedetti, M.G., Leardini, A., Banks, S.A., Cappello, A., Assirelli, D. and Catani, F. (2003) 'Fluoroscopic and gait analysis of the functional performance in stair ascent of two total knee replacement designs', *Gait Posture*, Vol. 17, pp.225–234.

Fregly, B.J., Sawyer, W.G., Harman, M.K. and Banks, S.A. (2005) 'Computational wear prediction of a total knee replacement from in vivo kinematics', *J. Biomech.*, Vol. 38, pp.305–314.

Halloran, J.P., Easley, S.K., Petrella, A.J. and Rullkoetter, P.J. (2005) 'Comparison of deformable and elastic foundation finite element simulations for predicting knee replacement mechanics', *J. Biomech Engr.*, Vol. 127, pp.813–818.

Hanson, G.R., Suggs, J.F., Freiberg, A.A., Durbhakula, S. and Li, G. (2006) 'Investigation of in vivo 6DOF total knee arthoplasty kinematics using a dual orthogonal fluoroscopic system', *J. Orthop. Res.*, Vol. 24, pp.974–981.

Hoff, W.A., Komistek, R.D., Dennis, D.A., Gabriel, S.M. and Walker, S.A. (1998) 'Three-dimensional determination of femoral-tibial contact positions under in vivo conditions using fluoroscopy', *Clin. Biomech. (Bristol, Avon)*, Vol. 13, pp.455–472.

Hsieh, H.H. and Walker, P.S. (1976) 'Stabilizing mechanisms of the loaded and unloaded knee joint', *J. Bone Joint Surg. Am.*, Vol. 58, pp.87–93.

Incavo, S.J., Johnson, C.C., Beynnon, B.D. and Howe, J.G. (1994) 'Posterior cruciate ligament strain biomechanics in total knee arthroplasty', *Clin. Orthop. Relat. Res.*, Vol. 309, pp.88–93.

Komistek, R.D., Scott, R.D., Dennis, D.A., Yasgur, D., Anderson, D.T. and Hajner, M.E. (2002) 'In vivo comparison of femorotibial contact positions for press-fit posterior stabilized and posterior cruciate-retaining total knee arthroplasties', *J. Arthroplasty*, Vol. 17, pp.209–216.

Li, G., Suggs, J., Hanson, G., Durbhakula, S., Johnson, T. and Freiberg, A. (2006) 'Three-dimensional tibiofemoral articular contact kinematics of a cruciate-retaining total knee arthroplasty', *J. Bone Joint Surg. Am.*, Vol. 88, pp.395–402.

Machan, S., Powell, A., Roger, G., Brazil, D. and Bobyn, D. (2004) 'Use of in vivo kinematics over standard gait curves in finite element analysis', *Trans ORS*, Vol. 29, p.0242.

Mahoney, O.M., Noble, P.C., Rhoads, D.D., Alexander, J.W. and Tullos, H.S. (1994) 'Posterior cruciate function following total knee arthroplasty. A biomechanical study', *J. Arthroplasty*, Vol. 9, pp.569–578.

Maruyama, S., Yoshiya, S., Matsui, N., Kuroda, R. and Kurosaka, M. (2004) 'Functional comparison of posterior cruciate-retaining versus posterior stabilized total knee arthroplasty', *J. Arthroplasty*, Vol. 19, pp.349–353.

Most, E., Zayontz, S., Li, G., Otterberg, E., Sabbag, K. and Rubash, H.E. (2003) 'Femoral rollback after cruciate-retaining and stabilizing total knee arthroplasty', *Clin. Orthop. Relat. Res.*, Vol. 410, pp.101–113.

Nozaki, H., Banks, S.A., Suguro, T. and Hodge, W.A. (2002) 'Observations of femoral rollback in cruciate-retaining knee arthroplasty', *Clin Orthop. Relat. Res.*, Vol. 404, pp.308–314.

Schmidt, R., Komistek, R.D., Blaha, J.D., Penenberg, B.L. and Maloney, W.J. (2003) 'Fluoroscopic analyses of cruciate-retaining and medial pivot knee implants', *Clin. Orthop. Relat. Res.*, Vol. 410, pp.139–147.

Simmons, S., Lephart, S., Rubash, H., Pifer, G.W. and Barrack, R. (1996) 'Proprioception after unicondylar knee arthroplasty versus total knee arthroplasty', *Clin. Orthop. Relat. Res.*, Vol. 331, pp.179–184.

Sorger, J.I., Federle, D., Kirk, P.G., Grood, E., Cochran, J. and Levy, M. (1997) 'The posterior cruciate ligament in total knee arthroplasty', *J Arthroplasty*, Vol. 12, pp.869–879.

Stiehl, J.B., Komistek, R.D., Dennis, D.A., Paxson, R.D. and Hoff, W.A. (1995) 'Fluoroscopic analysis of kinematics after posterior-cruciate-retaining knee arthroplasty', *J. Bone Joint Surg. Br.*, Vol. 77, pp.884–889.

Wada, M., Tatsuo, H., Kawahara, H., Sato, M. and Baba, H. (2001) 'In vivo kinematic analysis of total knee arthroplasty with four different polyethylene designs', *Artif. Organs*, Vol. 25, pp.22–28.

Walker, S.A. (2000) *Determination of TKA Contact Mechanics from In Vivo Kinematic Data*, Master's Thesis, Colorado School of Mines, Golden, CO.

Walker, S.A., Hoff, W., Komistek, R. and Dennis, D. (1996) ‘‘In vivo’ pose estimation of artificial knee implants using computer vision’, *Biomed Sci. Instrum.*, Vol. 32, pp.143–150.

Warren, P.J., Olanlokun, T.K., Cobb, A.G. and Bentley, G. (1993) ‘Proprioception after knee arthroplasty. The influence of prosthetic design’, *Clin Orthop. Relat. Res.*, Vol. 297, pp.182–187.

Yoshiya, S., Matsui, N., Komistek, R.D., Dennis, D.A., Mahfouz, M. and Kurosaka, M. (2005) ‘In vivo kinematic comparison of posterior cruciate-retaining and posterior stabilized total knee arthroplasties under passive and weight-bearing conditions’, *J. Arthroplasty*, Vol. 20, pp.777–783.